Acoustic Excitations in a Self-Assembled Block Copolymer Photonic Crystal

Augustine M. Urbas,[1,*] Edwin L. Thomas,[1] Hartmut Kriegs,[2] George Fytas,[2,3]
Raluca S. Penciu,[3] and Lefteris N. Economou[3]

[1]*Massachusetts Institute of Technology, Cambridge, Massachusetts, 02139*
[2]*Max Planck Institute for Polymer Research, P.O. Box 3148, 55128 Mainz, Germany*
[3]*FORTH (Institute of Electronic Structure and Laser), P.O. Box 1527, 71110 Heraklion, Greece*

(Received 24 May 2002; published 14 March 2003)

High resolution Brillouin light scattering can sensitively detect acoustic phonons in concentrated solutions of a high molecular weight poly(styrene-*b*-isoprene) symmetric copolymer in toluene. This block copolymer lamellar forming system also possesses a photonic stop band in the visible spectrum. Based on the low but finite contrast in mechanical properties between the styrene and isoprene components and taking into account the geometrical characteristics of the layered microstructure, we calculate the acoustic band structure and represent the observed acousticlike and opticlike phonons.

DOI: 10.1103/PhysRevLett.90.108302 PACS numbers: 83.80.Uv, 63.22.+m, 82.35.Jk

Self-organized materials have proven useful in making photonic crystals. Colloidal crystals [1], synthetic opals [2], and block copolymers [3] are examples of self-assembling systems used for photonics. Block copolymers have proven to be a flexible platform for tunable photonic materials [4]. They have the potential to confine light in novel ways due to their unique pattern forming capabilities. The combination of mechanical and physical properties typical of these materials can give rise to acoustic stop bands for phonon wavelengths commensurate to the photon wavelength of the photonic band gap in the material. Phononic crystals [5,6] and multilayer acoustic materials [7] have been the focus of recent investigations [8–11] and are being studied for a variety of applications [12,13]. Such materials are novel systems for the study of phonon-mediated light interactions such as stimulated Brillouin scattering. We have examined the acoustic and phonon spectral properties of concentrated block copolymer solutions using polarized Brillouin light scattering [14]. We study the acoustic properties of a lamellar forming block copolymer system in the hypersonic (GHz) frequency range. We report the first evidence of phonon spectral features characteristic of the morphology of the block copolymer.

The diblock copolymer used was prepared by sequential addition anionic polymerization. The polystyrene (S) block had a molecular weight of 480 kg/mole, the polyisoprene (I) block of 560 kg/mole and a polydispersity index of 1.02. The weight percent of styrene was 46% as determined by NMR, corresponding to a volume fraction of 0.44 polystyrene. The morphology of the material as cast from toluene was lamellar determined from thin OsO_4 stained sections examined by transmission electron microscopy. The concentrated polymer solutions were prepared by placing a prescribed amount of polymer into a 5 mm diameter, thin walled, glass, NMR tube (Wilmad Glass), followed by solvent, allowing the polymer to dissolve completely. The 17% solution was initially strongly green opalescent. The 30% concentration was obtained by allowing a portion of the solvent to evaporate. The second concentration was green-yellow opalescent. A second solution of 9% SI in toluene was prepared which had a weak bluish cast. The selective reflectivity of the highest two concentrations is indicative of the photonic stop band arising from the layered microstructure of the material.

The light scattering experiment was conducted using a frequency and intensity stabilized single mode solid state laser with a wavelength of $\lambda_0 = 532$ nm and a small bandwidth (10 MHz). The scattered light was analyzed at various specified angles, θ, with respect to the illuminating beam. The scattering wave vector is defined as $q = ||\mathbf{q}_i - \mathbf{q}_f|| = \frac{4\pi n}{\lambda_0}\sin(\frac{\theta}{2})$, where $\mathbf{q}_i$ and $\mathbf{q}_f$ are the wave vector of the incident and scattered light, respectively, and n is the average refractive index of the medium. The inelastically scattered light was focused onto the pinhole aperture of a tandem-Fabry-Perot interferometer (TFPI, Sandercock) [14] with a variable free spectral range. The TFPI was stabilized with a split weak laser beam, while passing the frequency of the elastic peak, allowing for long time measurement without loosing spectral sensitivity. In order to map the phonon dispersion relation of the block copolymer solution, scattering experiments were conducted for ten angles. For each scattering angle, the data consisted of a plot of the intensity of scattered light versus the frequency. Typical data are shown in Figs. 1(a) and 1(b) for 30% and Fig. 1(c) for the 9% SI polymer solution in toluene at $q = 0.025$ nm^{-1} ($\theta = 90°$).

The central (elastic) Rayleigh scattering peak is at the frequency of the incident beam. The inelastic light scattering represents photons with wave vector $\mathbf{q}$ scattered by interactions with phonons of wave vector $\mathbf{k}$. For homogeneous media, one Brillouin doublet at $\pm\omega$ appears only at $\mathbf{q} = \mathbf{k}$. The 17% SI solution displays two or three modes [Figs. 1(a) and 1(b)] depending on the cell orientation relative to the scattering wave vector $\mathbf{q}$. This is in contrast

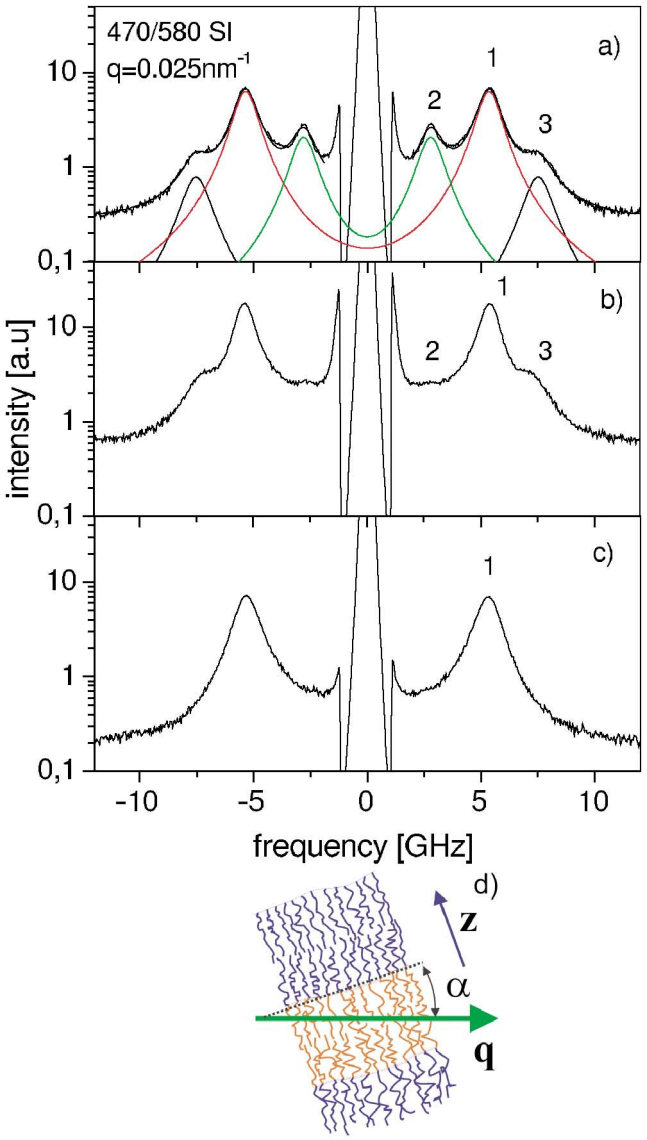

FIG. 1 (color). Rayleigh-Brillouin spectra obtained at $q = 0.025\ \mathrm{nm}^{-1}$ for 17% (b),(c) and 9% (a) SI solutions in toluene at 20 °C. (a) The rich phonon spectrum for 17% is represented by the superposition of three Lorentzians (solid lines). (b) The phonon spectrum of the same solution at a different orientation relative to the laser beam that affects only the intensity of the lowest phonon (2). The diagram, (d), shows schematically the orientation of the lamellar axis, z, relative to the light scattering wave vector q and the angle α between the lamellar plane and q. (c) Only the longitudinal phonon (1) is observed at low SI concentrations. The frequency region $\sim \pm 1$ GHz about the central peak is provided by the reference beam used for the stabilization of the tandem-FP interferometer. The numbers identify the modes: (1) is longitudinal mode, (2) is the "Bragg" mode, and (3) is the q-independent mode.

to the typical behavior for a fluid shown in Fig. 1(c) for the low concentration solution (9%). It exhibits one acoustic ($\omega \propto q$) longitudinal phonon $f = \frac{\omega}{2\pi} = 5.5$ GHz at $q = 0.025\ \mathrm{nm}^{-1}$ corresponding to an effective average medium. From the three Brillouin doublets of Fig. 1(a), cell rotation affects mainly the presence of the lowest frequency doublet (2.9 GHz). In the present polycrystalline high molecular weight SI solutions, momentum conservation requires $\mathbf{q} = \mathbf{G} + \mathbf{k}$, where the reciprocal one dimensional lattice vector $|\mathbf{G}| = \frac{2\pi}{d}$, with d being the lamellar spacing. The intensity of this "Bragg" phonon depends on the direction of q relative to the lamellar axis $\mathbf{z}$, being maximum for $\mathbf{q}$ parallel to $\mathbf{z}$ [Fig. 1(d)]. The resemblance to the Bragg diffraction conditions suggests the name of this new acoustic mode. Visual inspection of the sample shows large reflective grains, and the orientation dependence indicates that grains are of the order of the scattering volume (200 μm diameter). Conversely, peak (2) in Fig. 1(a) can (in the sense that $G \neq 0$) be utilized to determine directly the spacing d of the lamellar structure (see Fig. 3 below). This important system parameter can be inferred from the position of the reflectivity peak and can be directly measured only by ultrasmall angle scattering measurements in a solution.

The highest frequency phonon (3), also absent at low polymer concentrations, is a new mode and relates to the well ordered solutions. Cell rotation affects slightly the frequency of this mode [3%, Fig. 1(a)]. To elucidate the nature of this mode [(3) in Figs. 1(a) and 1(b)], we examine the inelastic light scattering at different scattering wave vectors. Figure 2 shows the spectra for 17% and 30% SI solutions in toluene at $q = 0.012\ \mathrm{nm}^{-1}$ and 20 °C. Modes (1) and (2) clearly vary with q, whereas the highest frequency phonon (3) shows negligible dispersion. The frequency of the Bragg mode (2) is found to decrease with SI concentration.

The positions of the Brillouin peaks as a function of q are plotted in Fig. 3. Mode (1) is the q dependent longitudinal phonon normally present in a homogeneous fluid. The insensitivity of $c = \frac{\omega}{q} (\cong 1370\ \frac{\mathrm{m}}{\mathrm{s}})$ to concentration changes in the examined range suggests low elastic constant contrast in the S and I sublayers swollen by the common solvent. The Bragg mode (2) in the present one dimensional structure is well described by

$$f = \frac{c}{d} - \frac{cq}{2\pi} \tag{1}$$

yielding directly d at the intercept $q = 0$. The fit of the above equation to the experimental data in Fig. 3 leads to $d = 168$ nm and $d = 192$ nm for the low and high concentration, respectively. A further check is the crossing of these two lines with the acoustic phonon which should occur at $q = \frac{\pi}{d}$, i.e., at the edge of the first Brillouin zone, as observed experimentally (arrows in Fig. 3).

The Bragg mode is characteristic of the lamellar spacing and allows us to measure accurately *in situ* this spacing d for each concentration by either the $q = 0$ or the crossing point. Prior to the scattering measurements a series of polymer solutions in toluene with concentrations between 5% and 60% by weight were made in NMR

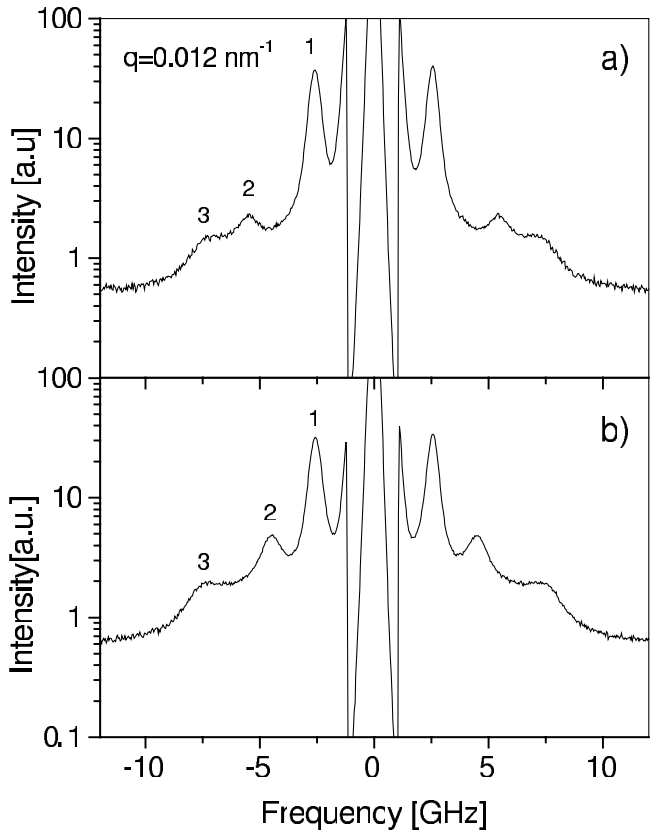

FIG. 2. Rayleigh-Brillouin spectra recorded at $q = 0.012\ \mathrm{nm}^{-1}$ for (a) 17% and (b) 30% SI solutions in toluene at 20 °C. The numbers identify the modes as in Fig. 1.

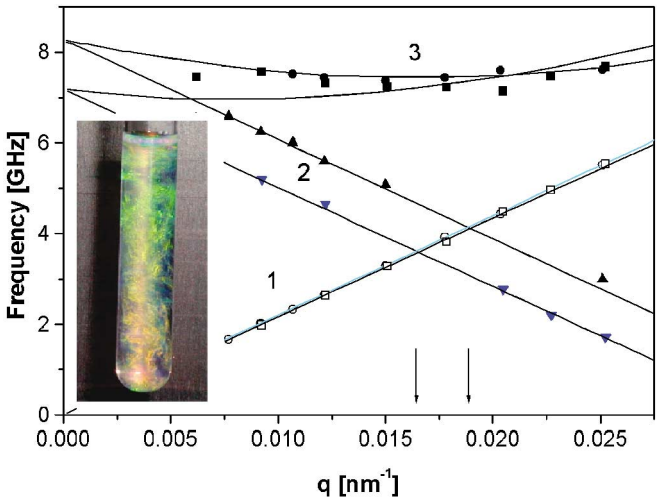

FIG. 3 (color). The phonon dispersion relations for the ordered SI solutions. The open circles and squares are, respectively, for the 17% and 30% SI solutions and the lines represent linear fits to the acoustic phonons. The solid circles and squares are for the opticlike mode for the 17% and 30% SI solutions, respectively. The Bragg mode (see text) is denoted by solid triangles 17% and solid inverted triangles 30%. The solid lines are computed from the dispersion relation for the lamellar spacings 168 and 192 nm, and show the acoustic, Bragg [Eq. (1)], and opticlike [Eq. (2)] phonons. The arrows on the horizontal axis indicate the edges of the first Brillouin zone in the two ordered SI solutions. This inset is a photograph of the ordered 17% solution. The granular reflective texture of the sample can be seen, as well as the shift in color due to the viewing angle of the lamellar grains.

tubes. Reflectivity measurements were taken from these solutions and a relationship between the lamellar spacing and the solvent volume fraction was extracted from the wavelengths of peak reflectivity for the samples. This relationship is linear in the range of concentrations examined and allows us to calculate the solvent volume fraction of each sample from the lamellar spacing.

The highest frequency mode (3) does not appreciably vary with q. The presence of the q-independent phonon at the frequency between 7–8 GHz can be attributed to a morphological mode with $\mathbf{k}$ almost parallel to the lamellar planes composed of two optically and mechanically different materials. (It is important to note that we would not expect to see this mode in the weakly segregated 9% solution because of the diffuse boundaries between the alternating layers.) To check this interpretation, we have calculated the phononic band structure of this medium following standard techniques [14–16]. The band diagrams for this material show three lower phonon modes, a longitudinal acoustic mode, a mode with "negative" dispersion [17] similar to our Bragg mode, and an opticlike mode. In the limit of small elastic contrast between the layers, we can estimate the frequencies of the allowed phonon modes by plotting the uniform solution $\omega = c|\mathbf{k}|$, where $|\mathbf{k}| = k_x\hat{\mathbf{x}} + k_y\hat{\mathbf{y}} + k_z\hat{\mathbf{z}}$ in the so called repeated zone scheme, i.e., by replacing k_z with $k_z - G$, where $G = \frac{2n\pi}{d}$ $(n = 0, 1, 2, 3, \ldots)$.

The relevant system parameters to complete the theoretical calculations are the density, longitudinal phase velocity, and the thickness of the S and I layers. The total lamellar repeat is extracted from the Bragg mode (2) in Fig. 3 and the fractional lamellar thickness can be taken to be that of the bulk block copolymer, 0.44 for the styrene layer, because toluene is a nonpreferential solvent for the two component blocks [18]. The lamellar spacing confirms the polymer concentration in the solution as well. To obtain reliable estimates of the sound velocity in the S and I layers and further calculate the effective c in the average medium, we have measured, by Brillouin scattering, the velocity of sound for a polystyrene (PS with 63 kg/mole) and a polyisoprene (PI with 10.5 kg/mole) solution in toluene over the whole concentration range [19]. We found that the commonly assumed ideal mixing for the compressibility M^{-1} (where $M = \rho c^2$ is the modulus and ρ is the density) overestimates M for both solutions [20]. The measured phase velocities at GHz frequencies for the I and S layers are as follows: for the 17% SI, $c_I = 1390\ \frac{\mathrm{m}}{\mathrm{s}}$, $c_S = 1400\ \frac{\mathrm{m}}{\mathrm{s}}$ and for the 30% SI ordered solution, $c_I = 1410\ \frac{\mathrm{m}}{\mathrm{s}}$, $c_S = 1450\ \frac{\mathrm{m}}{\mathrm{s}}$. Hence, the calculated effective c amounts to 1395 $\frac{\mathrm{m}}{\mathrm{s}}$ and 1430 $\frac{\mathrm{m}}{\mathrm{s}}$

for the 17% and 30% SI solutions, respectively. While the acoustic phonon in the 17% SI solution is in excellent agreement ($c = 1380\ \frac{\mathrm{m}}{\mathrm{s}}$ in Fig. 3) with the calculated c value, the latter is about 5% larger than the experimental value ($c = 1360\ \frac{\mathrm{m}}{\mathrm{s}}$ in Fig. 3). The observed softening of the acoustic phonon for the 30% SI solution might be due to relaxation effects.

As mentioned above, the low mechanical mismatch of the present one dimensional multilayers allows us to use the uniform dispersion $\omega = c|\mathbf{k}|$ with the replacement $k_z \rightarrow k_z - G$,

$$\omega = c\sqrt{(G - k_z)^2 + k_{xy}^2}, \tag{2}$$

where $k_z = q\sin\alpha$ and $k_{xy} = q\cos\alpha$ and α is the angle between $\mathbf{q}$ and the lamellar plane [see Fig. 1(d)]. For $\alpha = 90°$ we get both the acoustic mode (1) $\omega = cq$ (for $G = 0$) and the Bragg mode (2) $\omega = c(G - q)$ [see Eq. (1) for $G = \frac{2\pi}{d}$], with negative dispersion [17] as observed in our system. For $\alpha = 0°$ we get a third mode with weak dispersion beginning at $\omega = cG = \frac{2\pi c}{d}$. This is the opticlike phonon calculated in the band diagram and observed in our system (3). This mode is localized in the z direction within the layered structure present in the system. We can match the predicted, predominantly parallel to the lamellar planes, phonon mode to the observed opticlike phonon by adjusting the angle α. Using the physical parameters calculated above in our model and fitting α yields for the 17% concentration a matching phonon frequency at $\alpha = 15°$, and for the 30% concentration, at $\alpha = 26°$. The moderate sensitivity of the opticlike mode to the cell rotation as compared to the Bragg mode can result from the larger probability of finding q's in the parallel lamellar plane. In fact, the low α indicates that there is a preferential orientation of the grains along the axis of the cell rotation. The predicted opticlike mode in our dispersion relation can be brought into agreement with the observed q-independent Brillouin peak observed for both concentrations.

We conclude from the observed good theoretical description of the experimental dispersion relation that the rich phonon spectrum of layered structures can be a sensitive probe of the micromechanical properties and geometrical characteristics of ordered soft materials. Brillouin light scattering allows a direct and accurate access to the dispersion characteristics of wave propagation in mesoscopic structures as compared to the complementary inelastic x-ray scattering at shorter wavelengths and hence higher frequencies [21]. The wealth of the observed dispersion relations and consequently of the phonon group velocity opens up the possibility of controlling the directionality of phonon based energy flow by the light scattering geometry. We plan to extend this work by investigating the stimulated Brillouin scattering properties of this material for use as an active photonic medium.

*Electronic address: amurbas@elt.mit.edu

[1] S. Asher, J. Holtz, L. Liu, and Z. Wu, J. Am. Chem. Soc. **116**, 4997 (1994).
[2] A. Zakhidov, R. H. Baughman, Z. Iqbal, C. Cui, I. Khayrullin, S. O. Dantas, J. Marti, and V. G. Ralchenko, Science **282**, 897 (1998).
[3] A. C. Edrington *et al.*, Adv. Mater. **13**, 421 (2001).
[4] A. M. Urbas, R. Sharpe, Y. Fink, E. L. Thomas, M. Xenidou, and L. J. Fetters, Adv. Mater. **12**, 812 (2000).
[5] M. Sigalas and E. Economou, J. Sound Vib. **158**, 377 (1992).
[6] Z. Liu, X. Zhang, Y. Mao, Y. Y. Zhu, Z. Yang, C. T. Chang, and P. Sheng, Science **289**, 1734 (2000).
[7] R. Camley, B. Djafari-Rouhani, L. Dobrzynski, and A. Maraduin, Phys. Rev. B **27**, 7318 (1983).
[8] M. S. Kushwaha and B. Djafari-Rouhani, J. Appl. Phys. **80**, 3191 (1996).
[9] I. E. Psarobas, A. Modinos, R. Sainidou, and N. Stefanou, Phys. Rev. B **65**, 064307 (2002).
[10] A. Fainstein and B. Jusserand, Phys. Rev. B **54**, 11 505 (1996).
[11] R. Sprik and G. Wegdam, Solid State Commun. **106**, 77 (1998).
[12] J. Wang, D. C. Hutchings, A. Miller, E. W. V. Stryland, K. R. Welford, I. T. Muirhead, and K. L. Lewis, J. Appl. Phys. **73**, 4746 (1993).
[13] A. Diez, G. Kakarantzas, T. Birks, and P. S. J. Russel, IEEE Photonics Technol. Lett. **13**, 975 (2001).
[14] R. Penciu, G. Fytas, E. N. Economou, W. Steffen, and S. N. Yannopoulos, Phys. Rev. Lett. **85**, 4622 (2000).
[15] R. Penciu, M. Kafesaki, G. Fytas, E. Economou, W. Steffen, A. Hollingworth, and W. B. Russel, Europhys. Lett. **58**, 699 (2002).
[16] M. Kafesaki and E. N. Economou, Phys. Rev. B **60**, 11 993 (1999).
[17] Negative dispersion in the Bragg mode results from the transfer of the dispersion outside the first Brillouin zone.
[18] C. Huang, B. Chapman, T. Lodge, and N. Balsara, Macromolecules **31**, 9384 (1998).
[19] At these molecular weights both homopolymers have reached molecular weight independent glass transition temperatures and hence c values.
[20] Experimentally, $\frac{M_{\mathrm{toluene}}}{M_{\mathrm{PS/toluene}}} = 1 - 0.52\phi$ for volume fraction $0 \leq \phi \leq 0.3$ and $\frac{M_{\mathrm{toluene}}}{M_{\mathrm{PI/toluene}}} = 1 - 0.57\phi$ for $0 \leq \phi \leq 0.6$, where $M_{\mathrm{toluene}} = 1.59 \times 10^{10}\ \frac{\mathrm{dyne}}{\mathrm{cm}^2}$. Note that $M_{\mathrm{PS}} = 5.5 \times 10^{10}\ \frac{\mathrm{dyne}}{\mathrm{cm}^2}$ and $M_{\mathrm{PI}} = 4.6 \times 10^{10}\ \frac{\mathrm{dyne}}{\mathrm{cm}^2}$ for the bulk homopolymers. The experimental errors amount to 1%.
[21] S. Chen, C. Liao, H. Huang, T. Weiss, M. C. Bellisent, and F. Sette, Phys. Rev. Lett. **86**, 740 (2001).